

Enhancing the Thermal Efficiency of Longitudinally Finned Parabolic Trough Solar Receivers

Vinod Kumar^{1,*} , Stefano Savino¹ , and Carlo Nonino¹ 

¹University of Udine, Italy

*Correspondence: Vinod Kumar, kumar.vinod@spes.uniud.it

Abstract. The objective of this study was to investigate the conjugate heat transfer in a longitudinally finned parabolic trough solar thermal receiver tube, taking into account the non-uniform heat flux distribution along the tube circumference. Both smooth and longitudinally finned stainless steel receiver tubes, with Syltherm 800 oil as the heat transfer fluid, were numerically simulated using Ansys Fluent 2023R2 with periodic boundary conditions for Reynolds numbers ranging from 20,000 to 60,000. Two fin configurations were investigated in the study: two fins - of little practical interest but very useful to gain physical insight into the problem - and six fin receiver tubes. In addition, sub-cases within the two- and six-fin configurations were analyzed by varying the position and height of the fins. It was found that fins on the bottom side, exposed to a higher heat flux, mainly enhanced conduction, while fins on the top side mainly enhanced convection by directing higher velocity values toward the bottom side. To reduce hot spots and improve thermal efficiency, fins should be located in higher heat flux areas, and shorter fins on the bottom side and longer fins on the top side are recommended. Finally, the performance evaluation criteria were assessed using both the inner Nusselt number, based on the convective heat transfer coefficient as commonly reported in the literature, and an overall Nusselt number, based on the total heat transfer resistance of the receiver. For the most favorable two-fin and six-fin cases, the maximum temperature in the receiver decreased by a maximum of 16.7 K and 30 K, respectively.

Keywords: Parabolic Trough Receiver, Longitudinal Fins, Non-Uniform Heat Flux, Conjugate Heat Transfer

1. Introduction

Parabolic trough technology is one of the most widely used among other concentrating solar thermal technologies for both heating and power generation. This technology consists of a parabolic line focus collector, a receiver tube positioned at the focal line of the parabola, and a heat transfer fluid (HTF) flowing inside the receiver to absorb solar thermal energy [1].

The receiver, also called the absorber or heat collection element (HCE), is the main component of this technology. The receiver is a stainless-steel tube encased in a glass cover, and the annulus space is a vacuum-tight enclosure to reduce heat loss. The receiver is the most critical part of the system and can be susceptible to damage. As an example, receiver failure data is reported in [2]. Most failures are due to loss of vacuum, coating failures, and breakage of glass. This is often related to the non-uniform heat flux distribution, which leads to a temperature gradient around the receiver's circumference which may become very large at low HTF flow conditions, causing the tube to bend or deflect, potentially resulting in glass breakage. Most bending is within the elastic limit; however, higher temperature gradients may cause

plastic deformation in the receiver tube [3]. These failures will decrease the thermal efficiency of the receiver tube. In addition, the degradation of thermal oils used as HTF generates hydrogen gas, which slowly permeates through the receiver wall into the annulus space, causing thermal losses four times higher than in a proper vacuum enclosure [4-5].

To increase the reliability and lifespan of receivers, reducing the temperature gradient in the receiver circumference is the best option to overcome the above-listed problems. Various techniques have been studied to reduce the temperature gradient in the receiver, including inserts (fin [6], twisted tape [7], wire coil [8], ring [9], etc.), and porous media [10]. The main objective of these techniques is to reduce the receiver temperature, which leads to a reduction of thermal losses and an increase in thermal efficiency. A comprehensive literature review was conducted by Allam et al. [11].

The present study focuses on the behavior of longitudinal fins inside a parabolic trough receiver tube. Internally longitudinal finned parabolic receiver tubes have been extensively studied in the literature. Bellos et al. [12], numerically investigated the use of eight internal longitudinal rectangular fins with different thicknesses and heights. Increasing fin parameters leads to an increase in thermal performance but also increases pressure losses. Fins 10 mm in height and 2 mm thick are suggested as optimal, resulting in a 0.82% gain in thermal efficiency and a 13 K decrease in temperature gradient compared to a smooth receiver tube. Kurşun B. [13] examined longitudinal fins with flat and sinusoidal lateral surfaces; Nusselt number, thermal enhancement factor, and circumferential temperature difference were evaluated numerically. The use of sinusoidal fins decreases the maximum temperature by 48 K for a fluid inlet temperature of 500 K. As shown by Bellos and Tzivanidis [14], longitudinal fins with a reflector shield are the best choice for further enhancing thermal performance. Although a reflector shield reduces optical efficiency, the combination of internal fins and a reflector shield increases thermal efficiency. This technique is suitable for higher operating temperature conditions and allows for a 2.41 % increase in thermal efficiency and a 23K decrease in circumferential temperature. Adel et al. [15] found that fin height has a more pronounced influence than thickness. In their numerical analysis, five fins were inserted inside the bottom side of the receiver; fin height and thickness vary from 0 to 20 mm and from 0 to 8 mm, respectively. The results revealed that thermal efficiency improved by 8.45%. Liu et al. [16] showed that a larger velocity gradient improves convective heat transfer between HTF and receiver. At this aim, an inner tube is placed on the upper side to reduce heat losses, while straight fins are strategically placed on the lower side of the receiver with two HTFs (oil and water). An inner tube filled with low-temperature HTF (water) help reduce the temperature and outward heat flux on the top side of the receiver, while fins help reduce them on the bottom side. The Nusselt number increased by 2.28, and the maximum temperature decreased by up to 93.9 K.

In the existing literature, internal longitudinal fins within receiver tubes have been found to enhance thermal performance but have also resulted in increased pressure drop. Researchers have investigated different modifications to the finned receiver tube, with most studies focused on fundamental characteristics like fin height and width [12], [15]. However, the heat transfer mechanisms of longitudinal fins within the receiver have been little investigated, and there are no extensive studies on how the position of the fins affects the temperature gradient of the receiver surface due to the non-uniform distribution of the heat flux. Bellos et al. [17] conducted a study on the optimal number of fins within the receiver tubes. Different numbers of fins at different locations were studied. Using a multi-objective technique, they found that the receiver with three fins in the lower half was the optimal case, resulting in a 0.51% thermal efficiency gain. In general, it was concluded that using fins in the upper section does not significantly improve performance.

In this paper, the heat transfer mechanisms of fins on both top and bottom sides are analyzed. The location of the fins is optimized based on the maximum temperature and the circumferential temperature gradient. The characteristics of the velocity field, which can contribute to the enhancement of convective heat transfer, are also discussed. This investigation

builds upon the authors' previous work [18], in which the effects of a different number of fins (4 and 8) were analysed, and only the inner Nusselt number was taken into account.

2. System Description

This paper focuses on the receiver tubes of the LS-3 parabolic trough technology [19]. The main aim of this study is to investigate longitudinal fins' physical behavior in parabolic trough receiver tubes and to assess their effect on thermal performance. Three main configurations were numerically simulated, each representing different receiver geometries. The first consists of a smooth receiver without fins, as the reference case. The second and third feature receivers with two and six inner longitudinal fins and are named as 2F and 6F, respectively. Furthermore, the second and third configurations are subdivided into sub-cases that differ in the position and height of the fins, as shown in Figure 1a. The heat flux distribution on the receiver wall is shown in Figure 1b [10].

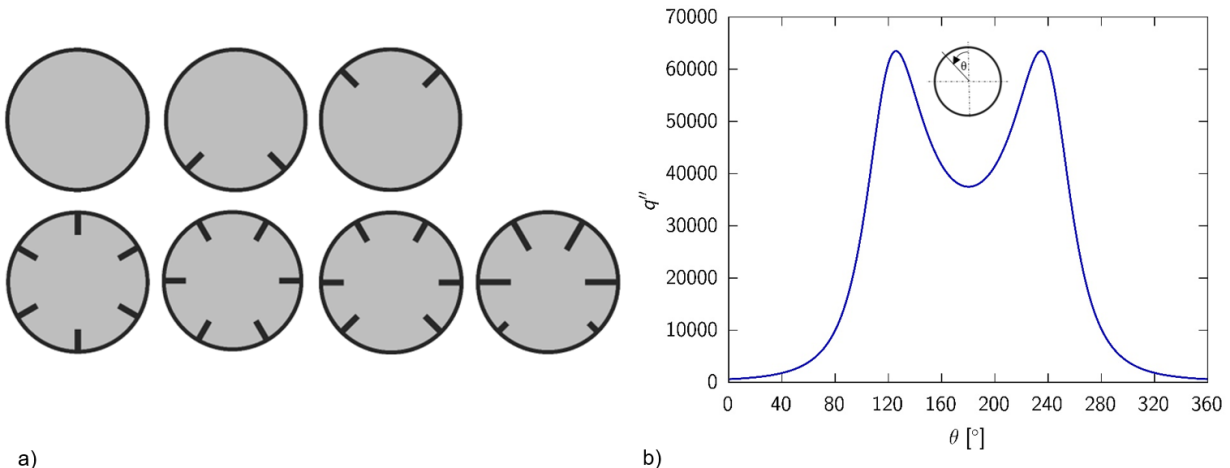


Figure 1. a) Cross section of the receiver tubes and b) heat flux distribution (q'') on the receiver wall

Table 1. Geometrical parameters of the receiver

	Smooth tube	2F Case1	2F Case2	6F Case1	6F Case2	6F Case3	6F Case4
D_i/D_o (mm) [19]	60/70	60/70	60/70	60/70	60/70	60/70	60/70
N	0	2	2	6	6	6	6
H (mm)	-	10	10	10	10	5-15	5-15
t (mm)	-	3	3	3	3	3	3

Table 2. Thermal properties of the receiver material and HTF fluid [13]

	Receiver (Stainless steel)	HTF (Syltherm 800)
ρ (kg/m ³)	8030	747.2
c_p (J/kg K)	502.5	1962
λ (W/m K)	24.9	0.0961
μ (Pa s)		0.00084

To speed up computations, a limited portion of the receiver of length L equal to D_o was investigated by imposing periodic inlet-outlet boundary conditions. In order to analyze only the effect of fin position and size without any other effects, the temperature dependence of the HTF properties was not considered in this study. The geometrical parameters of the receiver

are shown in Table 1, where D_i/D_o is the inner/outer diameter of the tube, N is the number of fins, H is the height, and t is the thickness of the fin. The fin thickness was kept constant in all simulations due to its limited effect [15]. The thermal properties of the receiver tube material and the HTF fluid are given in Table 2.

3. Numerical investigation

The numerical investigation of the steady, fully developed, turbulent flow was carried out using the finite volume method CFD tool Ansys Fluent 2023R2 [20]. Simulations were performed for Reynolds numbers ranging from 20,000 to 60,000, i.e. in the fully turbulent regime. A coupled solver was employed to enhance convergence. The second-order upwind scheme was adopted for the discretization of the governing equations and the SST $k-\omega$ model was used [10]. For the periodic boundary condition [8], a constant mass flow rate (0.871-2.61 kg/s, corresponding to the investigated Reynolds number range) and a constant upstream bulk temperature ($T_{in} = 500$ K) were assigned. The non-uniform heat flux distribution on the receiver outer wall was imposed using a user-defined expression. Radiative/convective heat losses were neglected in this study, to approximate the very high heat transfer resistance of the vacuum enclosure. Numerical analyses were carried out until the residual values for all solutions were less than 1e-10.

4. Processing of numerical data

In this study, the effects of inner longitudinal fins on pressure drop and heat transfer were investigated. HTF bulk temperature T_b , receiver wall temperature, and pressure gradient $\Delta P/L$ are the results of the numerical analyses.

The Reynolds number $Re = \rho v_{in} D_i / \mu$ was defined, as commonly done in the literature [13-16] using the receiver's inner diameter D_i as the reference length. ρ is the fluid density, v_{in} is the fluid inlet axial velocity, and μ is the dynamic viscosity.

The friction factor f was calculated as

$$f = \frac{(\Delta P/L)D_i}{\rho v_{in}^2/2} \quad (1)$$

The inner convective heat transfer coefficient was calculated, according to the prevailing approach in the literature [12-17], as

$$h_i = \frac{Q}{A_i(T_i - T_b)} \quad (2)$$

where Q is the total heat flux, A_i is the area of the inner actual surface, T_b is the fluid average bulk temperature, and T_i is the average temperature on the inner actual surface of the receiver. In this study, to evaluate the overall performance of the receiver and not just of its inner surface, the overall heat transfer coefficient h_o was also computed as

$$h_o = \frac{Q}{A_o(T_o - T_b)} \quad (3)$$

where A_o is the outer surface area, and T_o is the average temperature on the outer surface of the receiver.

The inner Nusselt number Nu_i is defined as

$$Nu_i = h_i D_i / \lambda \quad (4)$$

While the overall Nusselt number Nu_o is defined as

$$Nu_o = h_o D_o / \lambda \quad (5)$$

where λ is the thermal conductivity of the fluid.

Different solutions were compared by a performance evaluation criterion PEC for equal pumping power [21], calculated with both inner and overall Nusselt numbers, respectively:

$$PEC_i = (Nu_i / Nu_{i,0}) / (f / f_0)^{1/3} \quad (6)$$

$$PEC_o = (Nu_o / Nu_{o,0}) / (f / f_0)^{1/3} \quad (7)$$

where $Nu_{i,0}$ and $Nu_{o,0}$ represent the inner and overall Nusselt number of smooth tubes, respectively, while f and f_0 represent the friction factors for the finned tubes and smooth tubes, respectively.

5. Grid independence test and model validation

For the whole computational domain, a hexahedral conformal mesh was generated. Using the Ansys meshing tool, five distinct meshes were created for the case with six identical fins (6FCase2) to choose a suitable mesh. Each mesh had 30% more elements compared to the previous one. The maximum temperature, pressure gradient, and mean outer and inner actual surface temperatures of the receiver were computed at the highest Reynolds number. If the above parameters had a maximum fluctuation of less than 2%, the solution was considered mesh-independent. The final mesh used for the simulations consists of 164,300 elements and is shown in Figure 2b.

The validation of the Nusselt number and friction factor for the smooth receiver tube, using the Gnielinski [22] and Blasius correlations [23], respectively, is presented in Figure 2a. Overall, there was relatively little difference between the simulation and theoretical results, with average differences of 0.1% for the friction factor and 1.6% for the Nusselt number.

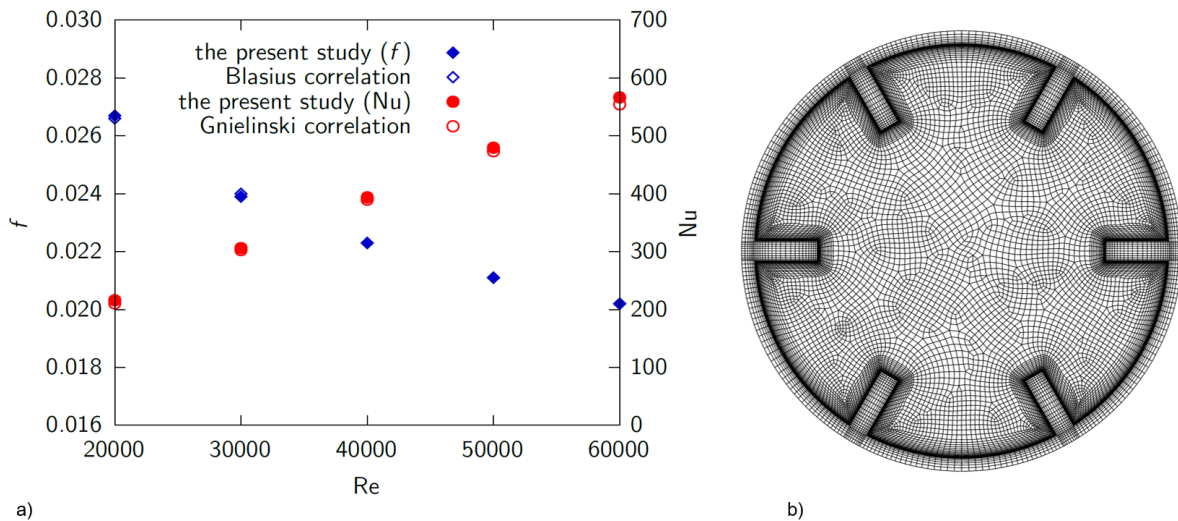


Figure 2. a) Comparison of friction factor & Nusselt number with correlations for smooth tubes and b) detail of the final mesh on a cross-section of the computational domain

6. Results and Discussion

The seven receiver geometries in Figure 1a were numerically analyzed for Reynolds numbers in the range of 20,000-60,000. Qualitative results, i.e., temperature contours, temperature profiles on the receivers' outer surface, and quantitative results, i.e., maximum temperatures,

Nusselt numbers, friction factors, and performance evaluation criteria, are presented in the following subsections.

6.1 Velocity and temperature fields

Temperature distributions and axial velocity profiles at the mid-section of the computational domain are displayed in Figure 3 for each investigated geometry and for the intermediate value of $Re=40,000$, corresponding to a mass flow rate of 1.74 kg/s. The white contours are axial velocity values equal to 0.65, 0.75 and, 0.85 m/s, respectively, while the position of the white cross marks the point of maximum velocity.

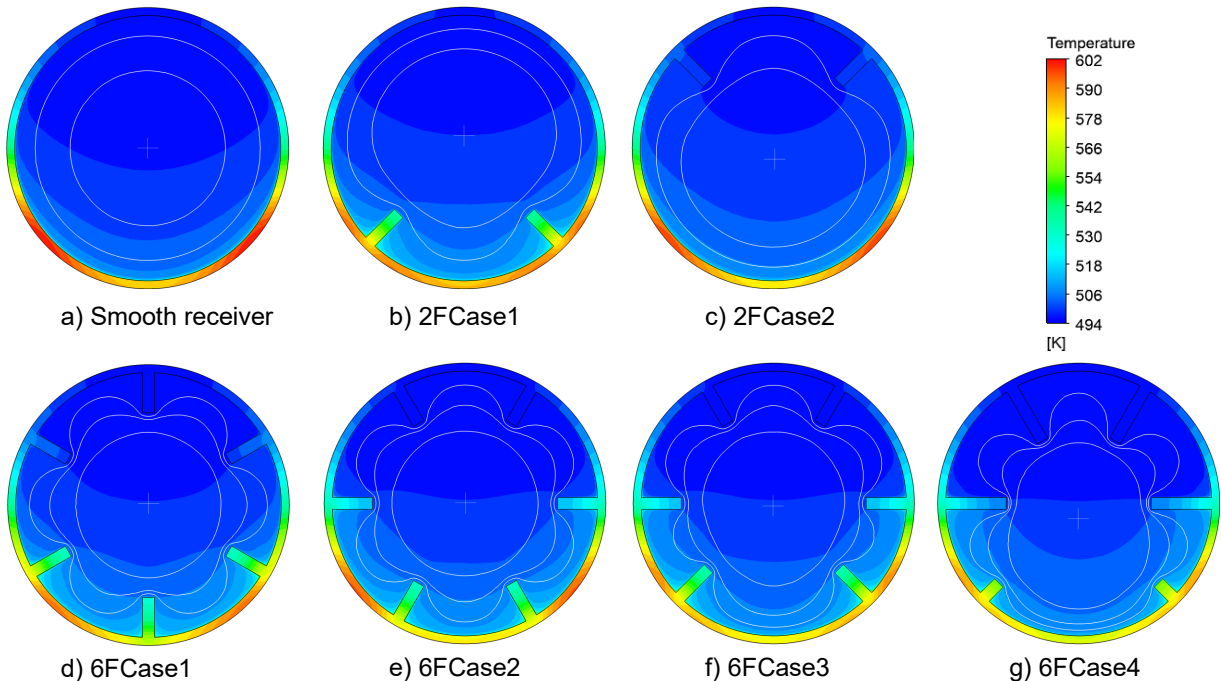


Figure 3. Temperature contours on the middle section of the computational domain for $Re = 40,000$

From the two fin cases, it is clear that fins on the bottom side reduce the temperature gradient in the receiver circumference, while fins on the top side increase the velocity gradient toward the bottom (hotter) side. In other words, fins on the bottom side greatly enhance heat conduction in the solid and thus convection to the colder fluid. Conversely, fins on the top side have little thermal effect because their temperature is very close to that of the surrounding fluid, but they do promote convective heat transfer by pushing the bulk of the fluid toward the hottest side. By combining these two effects, the overall heat transfer can be further enhanced, as demonstrated by the 6 fin configurations.

From the axial velocity profiles, it is observed that for smooth and symmetrically positioned fins (6FCase1 & 6FCase2), the core region has a very regular and smooth profile compared to other cases. Interfin space and fin height affect the local velocity near the wall; larger interfin space and shorter fin height on the bottom side and larger fin height on the top side increase the local velocity near the wall of the hot side, as shown for case 6FCase 4 in Figure 3g.

Fin placement plays a very important role in smoothing the temperature gradient in the receiver tube. To reduce the temperature gradient, fins must be positioned in areas of higher heat flux, as shown in Figure 3f. Additionally, shorter fins on the bottom side and longer fins on the top side not only decrease the temperature gradient in the receiver tube but also in the heat transfer fluid, as shown in Figure 3g.

The temperature contours in Figure 3 are consistent with the temperature distribution on the outer surface of the receiver tube for smooth, two-fin, and six-fin cases shown in Figures 4a and 4b. As can be seen, for the two-fin case, fins on the bottom side provide a lower maximum temperature, as well as case 4 for the six-fin case, where the optimal combination of fin position and height on top and bottom sides is adopted.

Figure 5 illustrates the maximum temperature of the receiver tube as a function of the Reynolds number. As the Reynolds number increases, the maximum temperature decreases. Cases with optimal fin locations (2FCase2 and 6FCase3) exhibit lower maximum temperatures. Furthermore, in cases with optimal fin locations, longer fins on the upper side and shorter fins on the lower side result in a greater decrease in the maximum temperature.

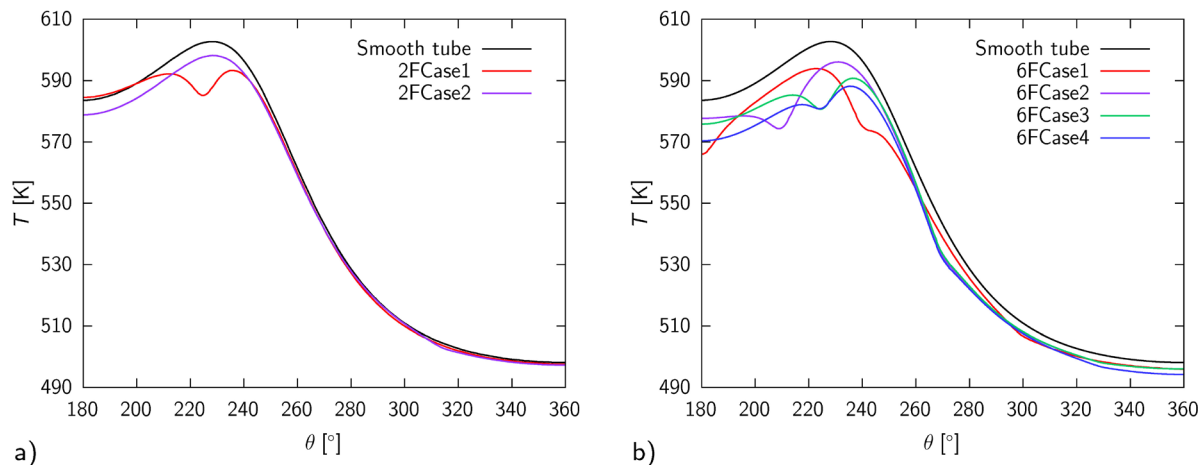


Figure 4. Receiver outer wall circumferential temperature distribution for $Re = 40,000$ for a) two fin and b) six fin cases

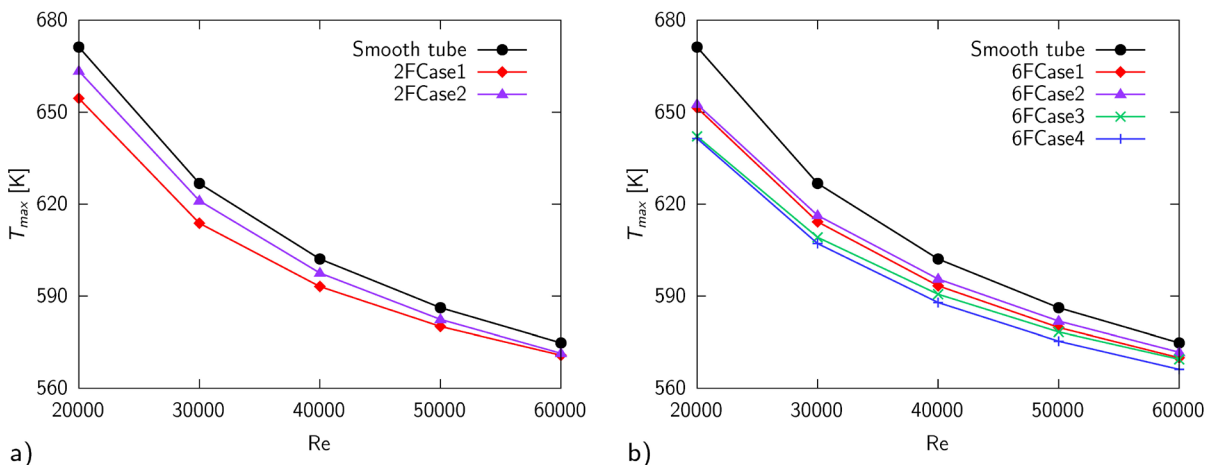


Figure 5. Variation of the maximum temperature (T_{max}) with Re for a) two-fin and b) six-fin cases

6.2 Performance parameters

The performance of the receiver geometries was investigated at different Reynolds numbers ranging from 20.000 to 60.000, corresponding to HTF mass flow rates in the range 0.871-2.61 kg/s. The results are shown in Figure 6 in terms of friction factor and Nusselt number. The addition of fins, as well as increasing the Reynold number, increases both the friction factor and the Nusselt number. For example, as can be seen in Figure 6b, the friction factor for 6FCase 4 increased by 1.87 times compared to the smooth tube. Regarding the Nusselt number, Nu_o is plotted in Figures 6c and 6d, and Nu_i in Figures 6e and 6f.

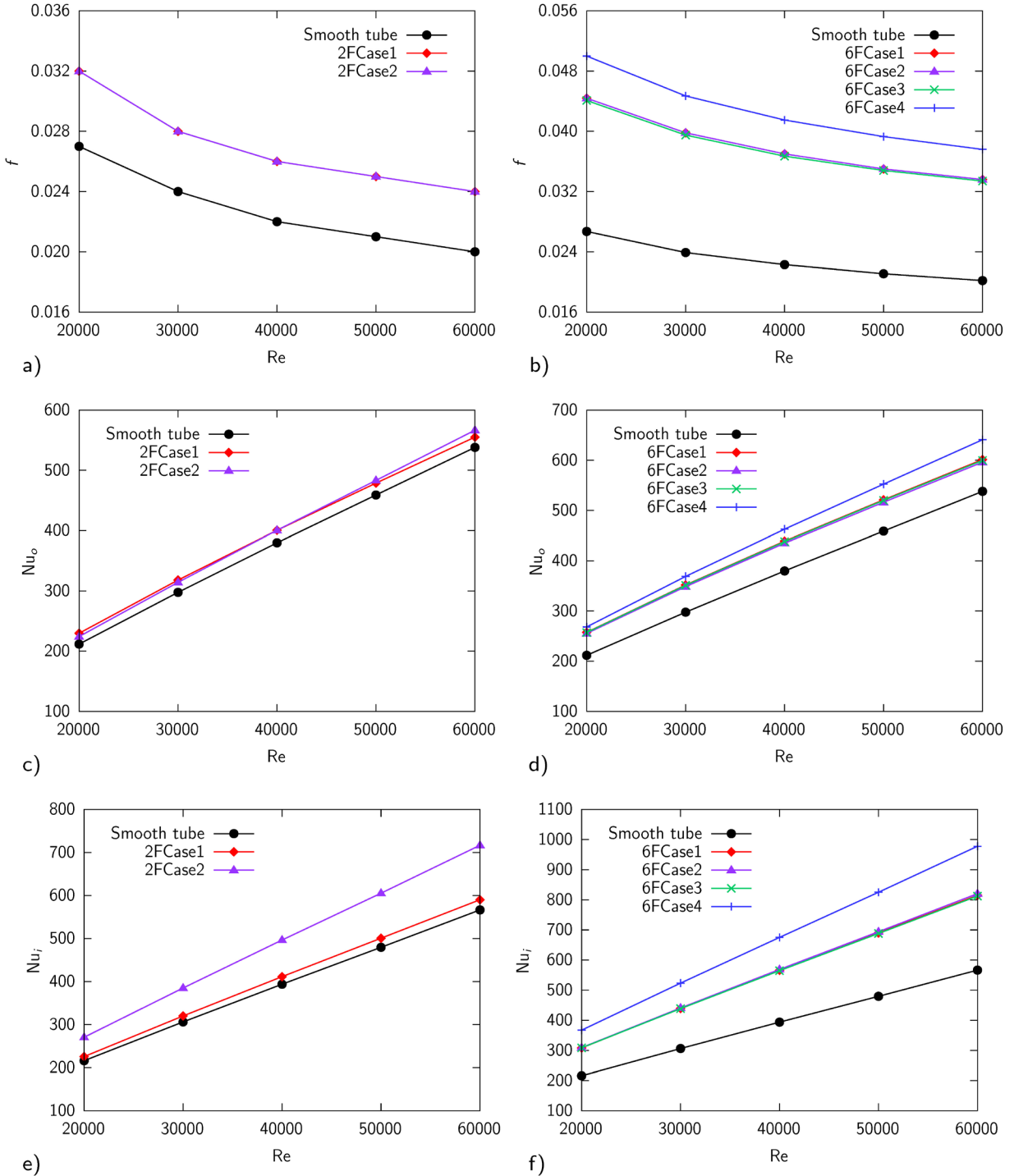


Figure 6. Variation of f , Nu_o , and Nu_i with Re for two-fin and six-fin cases

As can be seen, Nu_i is larger than Nu_o , and for the two-fin cases Nu_i is larger for 2F Case 2 (fins on the cold side) than for 2F Case 1 (fins on the hot side). This is because in 2F Case 2, as already mentioned, the fin temperature is very close to that of the fluid and, as a consequence, the average temperature on the inner actual surface of the receiver T_i in equation 2 becomes smaller, giving a higher Nusselt number. However, since we are interested in the overall performance of the receiver, the thermal losses are related to the external temperature and therefore we should refer to the overall Nusselt number Nu_o . For low Reynolds numbers, Nu_o is slightly larger for 2F Case 1 than for 2F Case 2, because the effect of conduction in the fins plays a more significant role. For higher Reynolds numbers we see the opposite, as convection effects become more relevant.

The performance evaluation criteria based on the overall Nusselt number (PEC_o) is shown in Figures 7a and 7b, and the performance evaluation criteria based on the inner Nusselt number (PEC_i) is shown in Figures 7c and 7d. As expected, case 6FCase4 provides the best performance. As can be clearly seen, the two approaches can lead to different performance evaluations, as is particularly evident in the case of the two fins, which is of little practical interest but very useful for getting a physical insight into the problem. From Figure 7c, it seems that the solution with fins on the cold side (2FCase2) performs much better than the one with fins on the hot side (2FCase1). This is in contrast to Figure 4a, as we are interested in the performance of the whole receiver and not just in its internal convection coefficient. It can be concluded that if the fins are not placed symmetrically inside the receiver and due to the non-uniform heat flux distribution, the performance evaluation of solar receivers should be assessed based on their outer surface temperature, i.e. with reference to an overall Nusselt number Nu_o .

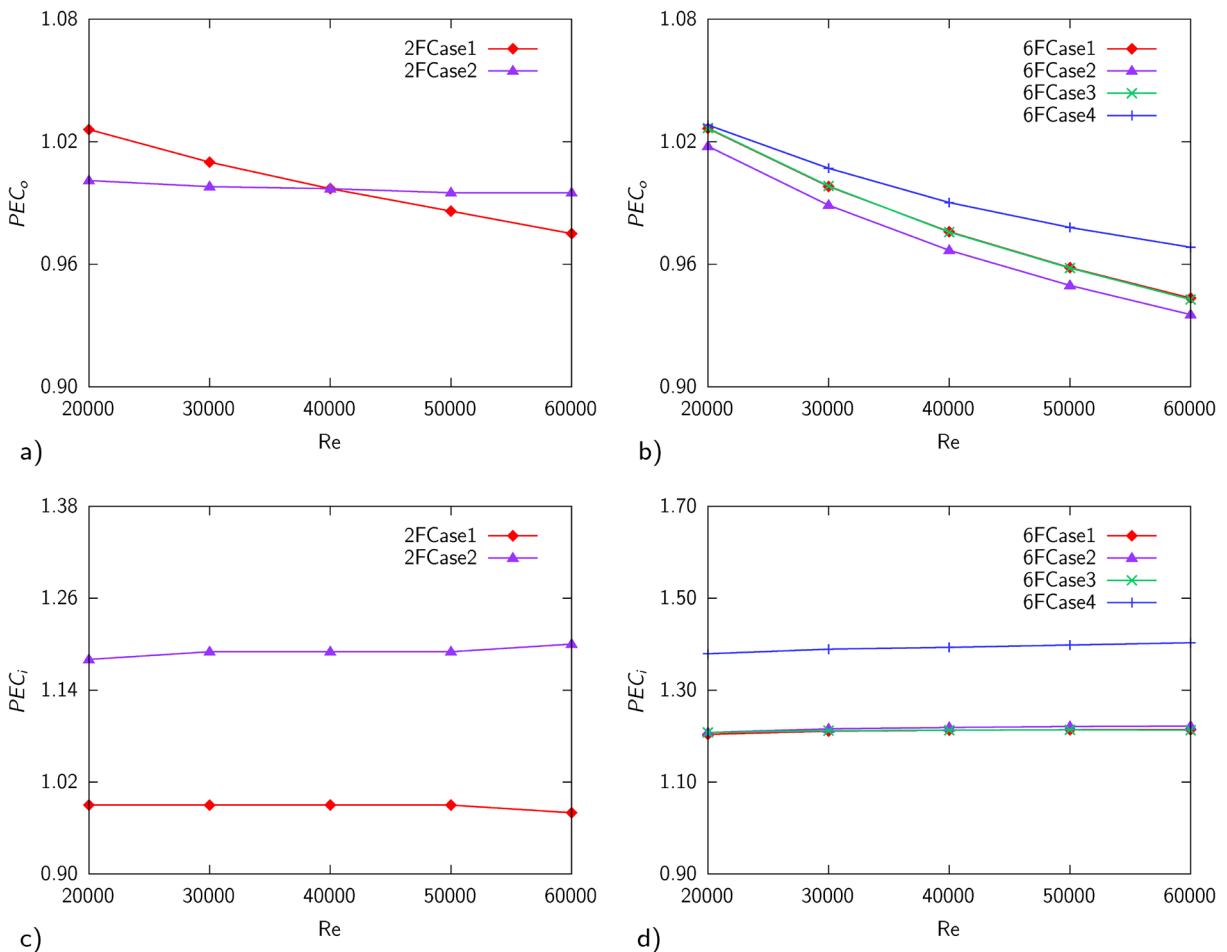


Figure 7. Variation of PEC_o and PEC_i with Re for two-fin and six-fin cases

7. Conclusions

In this study, the conjugate heat transfer in a longitudinally finned parabolic trough solar thermal receiver was numerically analyzed. The purpose was to reduce the intensity of hotspots, thereby minimizing the probability of failure, and to investigate the different heat transfer mechanisms enhanced by fins on the heated and unheated sides of the receiver. The two-fins, of little practical interest but very useful to gain physical insight into the problem, and the six-fins receiver tubes were analyzed, together with the smooth channel as a reference case. In order to account for the non-uniform heat flux distribution and the non-symmetrical arrangement of the fins, the thermal performance was evaluated in terms of both an inner - according to the

prevailing approach in the literature - and an overall Nusselt number. The following main conclusions are summarised.

- Fins exhibit different behaviors on the bottom side compared to the top side. Fins on the bottom side decrease the receiver circumferential temperature gradient, while fins on the top side increase the HTF velocity gradient towards the bottom (hotter) side.
- To reduce circumferential temperature gradient, fins must be positioned in areas of higher heat flux.
- For smooth and symmetrically positioned fins, the core region exhibits a very smooth axial local velocity profile. Larger interfin space, shorter fin height on the bottom side and larger fin height on the top side increase local velocity near the wall.
- For the most effective fin size and positioning (2FCase1 and 6FCase4), the highest circumferential temperature gradient decreased by 16.7 K and 30 K for the two-fin and the six-fin case, respectively.
- PEC_o decreases with an increase in Re , but PEC_i , approximately remains constant.
- For overall performance evaluation, finned receiver tubes should be assessed based on their outer surface temperature.

Data availability statement

Data can be requested from the authors.

Author contributions

Vinod Kumar contributed to the conceptualization, investigation, software, methodology, data analysis, formal analysis, original draft writing, and visualization. Stefano Savino was involved in the investigation, methodology, resource management, formal analysis, and manuscript review and editing. Carlo Nonino contributed to the investigation, methodology, technical discussions, formal analysis, and manuscript review and editing.

Competing interests

The authors declare no competing interests.

References

- [1] H. Price, E. Lüpfert, D. Kearney, E. Zarza, G. Cohen, R. Gee, and R. Mahoney, "Advances in Parabolic Trough Solar Power Technology," *J. Sol. Energy Eng.*, vol. 124, no. 2, pp. 109–125, May 2002, doi: [10.1115/1.1467922](https://doi.org/10.1115/1.1467922).
- [2] H. Price, M. J. Hale, R. Mahoney, C. Gummo, R. Fimbres, R. Cipriani, "Developments in High Temperature Parabolic Trough Receiver Technology," *Proc. ISEC*, vol. 2004, pp. 659–667, Dec. 2004, doi: [10.1115/ISEC2004-65178](https://doi.org/10.1115/ISEC2004-65178).
- [3] H. Price, R. Forristall, T. Wendelin, A. Lewandowski, T. Moss, C. Gummo, "Field Survey of Parabolic Trough Receiver Thermal Performance," *Proc. ISEC*, pp. 109-116, 2006, doi: [10.1115/ISEC2006-99167](https://doi.org/10.1115/ISEC2006-99167).
- [4] J. Li, Z. Wang, D. Lei, J. Li, "Hydrogen permeation model of parabolic trough receiver tube," *Sol. Energy*, vol. 86, no. 5, pp. 1187-1196, May 2012, doi: [10.1016/j.solener.2012.01.011](https://doi.org/10.1016/j.solener.2012.01.011).
- [5] L. Moens, D. M. Blake, "Mechanism of Hydrogen Formation in Solar Parabolic Trough Receivers," *NREL Report*, no. 42881, pp. 1–10, 2008.
- [6] E. Bellos, C. Tzivanidis, and D. Tsimpoukis, "Thermal enhancement of parabolic trough collector with internally finned absorbers," *Sol. Energy*, vol. 157, pp. 514–531, Aug. 2017, doi: [10.1016/j.solener.2017.08.067](https://doi.org/10.1016/j.solener.2017.08.067).

- [7] Sh. Ghadirijafarbeigloo, A.H. Zamzamian, M. Yaghoubi, "3-D Numerical Simulation of Heat Transfer and Turbulent Flow in a Receiver Tube of Solar Parabolic Trough Concentrator with Louvered Twisted-tape Inserts," *Energy Procedia*, vol. 49, pp. 373-380, 2014, doi: [10.1016/j.egypro.2014.03.040](https://doi.org/10.1016/j.egypro.2014.03.040).
- [8] İ. H. Yilmaz, A. Mwesigye, T. T. Göksu, "Enhancing the overall thermal performance of a large aperture parabolic trough solar collector using wire coil inserts," *Sustain. Energy Technol. Assess.*, vol. 39, 2020, doi: [10.1016/j.seta.2020.100696](https://doi.org/10.1016/j.seta.2020.100696).
- [9] K. A. Ahmed, E. Natarajan, "Thermal performance enhancement in a parabolic trough receiver tube with internal toroidal rings: A numerical investigation," *Appl. Therm. Eng.*, vol. 162, 2019, 114224, doi: [10.1016/j.aplthermaleng.2019.114224](https://doi.org/10.1016/j.aplthermaleng.2019.114224).
- [10] P. Wang, D.Y. Liu, C. Xu, "Numerical study of heat transfer enhancement in the receiver tube of direct steam generation with parabolic trough by inserting metal foams," *Appl. Energy*, vol. 102, pp. 449-460, 2013, doi: [10.1016/j.apenergy.2012.07.026](https://doi.org/10.1016/j.apenergy.2012.07.026).
- [11] M. Allam, M. Tawfik, M. Bekheit, E. El-Negiry, "Heat transfer enhancement in parabolic trough receivers using inserts: A review," *Sustain. Energy Technol. Assess.*, vol. 48, 2021, 101671, doi: [10.1016/j.seta.2021.101671](https://doi.org/10.1016/j.seta.2021.101671).
- [12] E. Bellos, C. Tzivanidis, D. Tsimpoukis, "Multi-criteria evaluation of parabolic trough collector with internally finned absorbers," *Appl. Energy*, vol. 205, pp. 540-561, 2017, doi: [10.1016/j.apenergy.2017.07.141](https://doi.org/10.1016/j.apenergy.2017.07.141).
- [13] B. Kurşun, "Thermal performance assessment of internal longitudinal fins with sinusoidal lateral surfaces in parabolic trough receiver tubes," *Renew. Energy*, vol. 140, pp. 816-827, 2019, doi: [10.1016/j.renene.2019.03.106](https://doi.org/10.1016/j.renene.2019.03.106).
- [14] E. Bellos, C. Tzivanidis, "Enhancing the performance of a parabolic trough collector with combined thermal and optical techniques," *Appl. Therm. Eng.*, vol. 164, 2020, 114496, doi: [10.1016/j.aplthermaleng.2019.114496](https://doi.org/10.1016/j.aplthermaleng.2019.114496).
- [15] A. Laaraba, G. Mebarki, "Enhancing Thermal Performance of a Parabolic Trough Collector with Inserting Longitudinal Fins in the Down Half of the Receiver Tube," *J. Therm. Sci.*, vol. 29, pp. 1309–1321, Apr. 2020, doi: <https://doi.org/10.1007/s11630-020-1256-8>.
- [16] P. Liu, T. Ren, Y. Ge, W. Liu, L. Chen, "Performance analyses of a novel finned parabolic trough receiver with inner tube for solar cascade heat collection," *Sci. China Technol. Sci.*, vol. 66, pp. 1417–1434, 2023, doi: [10.1007/s11431-022-2201-3](https://doi.org/10.1007/s11431-022-2201-3).
- [17] E. Bellos, C. Tzivanidis, D. Tsimpoukis, "Optimum number of internal fins in parabolic trough collectors," *Appl. Therm. Eng.*, vol. 137, pp. 669-677, 2018, doi: [10.1016/j.aplthermaleng.2018.04.037](https://doi.org/10.1016/j.aplthermaleng.2018.04.037).
- [18] V. Kumar, S. Savino, C. Nonino, "Effect of height and position of inner rectangular longitudinal fins in parabolic trough solar receivers," *Comput. Therm. Sci.: An Int. J.*, vol. 17 (3), pp. 1–11, 2025, doi: [10.1615/ComputThermalScien.2024055167](https://doi.org/10.1615/ComputThermalScien.2024055167).
- [19] A. Fernández-García, E. Zarza, L. Valenzuela, M. Pérez, "Parabolic-trough solar collectors and their applications," *Renew. Sustain. Energy Rev.*, vol. 14, no. 7, pp. 1695-1721, Jul. 2010, doi: [10.1016/j.rser.2010.03.012](https://doi.org/10.1016/j.rser.2010.03.012).
- [20] ANSYS, Inc. 2023 Ansys Fluent Theory Guide, release 2023R2.
- [21] R.L. Webb and E.R.G. Eckert, "Application of rough surfaces to heat exchanger design," *Int. J. Heat Mass Transf.*, vol. 15, no. 9, pp. 1647–1658, Sep. 1972, doi: [10.1016/0017-9310\(72\)90095-6](https://doi.org/10.1016/0017-9310(72)90095-6).
- [22] Gnielinski V. New equations for heat and mass transfer in turbulent pipe and channel flow. *Int Chem Eng* 1976; 16:359–68.
- [23] Blasius H. Das Aehnlichkeitsgesetz bei Reibungsvorgängen in Flüssigkeiten, *Mitteilungen über Forschungsarbeiten auf dem Gebiete des Ingenieurwesens*, 131; 1913.